Published in final edited form as:
Acta Neurol Scand. 2010 March 1; 121(3): 209. doi:10.1111/j.1600-0404.2009.01188.x.

Arterial Spin Labeling Demonstrates that Focal Amygdalar Glutamatergic Agonist Infuasion Leads to Rapid Diffuse Cerebral Activation

Jeeva P Munasinghe[1], **Madhumita Banerjee**[2], **Maria T Acosta**[2,3], **Melissa Banks**[2], **Alison Heffer**[1,4], **Alfonso C. Silva**[1], **Alan Koretsky**[1], and **William H Theodore**[3]

[1] MRI Research Facility, National Institutes of Health, Bethesda, MD, USA

[2] Epilepsy Research Section, National Institutes of Health, Bethesda, MD, USA

[3] Clinical Epilepsy Section, National Institute of Neurological Disorders and Stroke, National Institutes of Health, Bethesda, MD, USA

[4] National Institute of Child Health and Human Development, National Institutes of Health, Bethesda, MD, USA

Abstract

Objectives—To investigate acute effects of intra-amygdalar excitatory amino acid administration on blood flow, relaxation time and apparent diffusion coefficient in rat brain.

Materials and Methods—Several days after MR-compatible cannula placement in right basolateral amygdala, anesthetized rats were imaged at 7T. Relative CBF was measured before and 60 minutes after infusion of 10 nanomoles KA, cAMPA, ATPA, or normal saline using arterial spin labeling. Quantitative T_2 and diffusion weighted images were acquired. rCBF, T_2 and ADC values were evaluated in bilateral basolateral amygdala, hippocampus, basal ganglia, frontal and parietal regions.

Results—KA led to the highest, and ATPA lowest bilateral rCBF increases. Time courses varied among drugs. T_2 for KA and AMPA was higher while ADC was lower for KA.

Conclusions—Intraamygdalar injection of GluR agonists evoked bilateral seizure activity and increased rCBF, greater for KA and AMPA than selective ATPA GluR5 activation.

Keywords

glutamate receptors; KA; ATPA; AMPA; MRI; CBF; seizures

Introduction

There are three known brain ionotropic glutamate receptor (GluR) types, n-methyl-d-aspartate (NMDAr), α-amino-3-hydroxy-5-methylisoxazole-4- propionic acid (AMPAr) and Kainic acid (KAr). NMDA receptors are known to play a role in slower, longer-lasting excitatory processes, while AMPAr and KAr may subserve faster excitatory processes (1). KA acts as a powerful convulsant in the CNS even at low concentrations and has served as an animal model of human temporal lobe epilepsy (2). KA activates AMPA receptors as well. ATPA ((RS-2-

Address Correspondence to: William H Theodore MD., National Institute for Neurological Disorders and Stroke/National Institutes of Health, Building 10 Room 5N-250, Bethesda MD 20892 USA, Phone: 301-402-1505, FAX: 301-402-2871, Theodorw@ninds.nih.gov.

amino-3-(3-hydroxy-5-tert-butylisoxazole-4-yl) propionic acid) is an experimental compound that was originally synthesized as an AMPA analog but has since been shown to activate preferentially the KAr GluR5 subtype (3). GluR5, with high density in the basolateral nucleus, is involved in regulation of amygdala and hippocampal function (4).

The relative contribution of GluR receptor subtypes to epileptogenesis and seizure expression is uncertain (2). Several lines of evidence suggest that GluR5 receptors have a prominent role in the regulation of neuronal excitability in the amygdala, and are related to epileptogenesis (5). Up regulation of metabotropic GluR5 receptors has been reported in hippocampal resections from patients with TLE (6). Other studies suggest that GluR5 receptors may play a less important role (2).

Relative effects of GluR subtype activation can be assessed by measuring cerebral blood flow (CBF), a key marker for clinical seizures. Studies using 14C-iodoantipyrine in rats given electroshock seizures showed flow increases of up to 400% (7). Arterial spin labeling (ASL) techniques (8) provide a powerful non-invasive method (9) for obtaining quantitative rCBF with no external contrast agent.

A number of studies have reported abnormalities in qualitative and/or quantitative changes in T_2 or diffusion (ADC) signal intensities and/or values (10) after GluR activation. Reduced ADC has been shown in prolonged human focal status epilepticus (11) (12). Patients studied 4 to 24 hours after complex partial status epilepticus (CPSE) onset due to a variety of pathologic insults showed regional hyperintensity on diffusion-weighted imaging (DWI), and a reduction of ADC (13). Some studies have reported that the DWI hyperintense signal after prolonged CPSE, are more extensive than T_2-weighted signal increase (14). Changes in inherent relaxation and diffusion coefficients may reflect changes in brain microscopic environment immediately after drug administration.

In order to help elucidate the physiological and structural effects of status epilepticus, and the potential role of GluR subtypes, we compared the effects of intramygdalar (*i.a.*) administration of KA, AMPA, ATPA and saline on acute rCBF, T_2 and ADC values in rat brain. We used intravenous (*i.v.)* KA to help control for the effects of cannula placement in *i.a.* rats.

Methods

All studies were performed in compliance with the guide for the care and use of Laboratory Animal Resources (1996), National Research Council, and approved by the NINDS Animal Care and Use Committee. Male Sprague-Dawley rats weighing approximately 250 grams, anesthetized with ketamine/xylocine, had a single internal MR-compatible Teflon cannula (28 gauge tube, *i.d.* 0.15 mm, Plastics One, Inc. Roanoke, VA. USA.) placed stereotactically in right basolateral amygdala 2.8 mm posterior to the Bregma. After 7–10 days rest, rats were anesthetized with 1.5% isoflurane/air mixture, intubated, and placed on a mechanical ventilator (SAR/830/P, CWE, Inc. model, PA. USA.). Lines were placed in femoral artery to monitor blood pressure, and femoral vein for drug and fluid administration. Intubation was essential because a bolus of 3 mg/kg (2 mg/ml solution; 0.375 ml for a 250 gm rat) Pancuronium bromide was administered to paralyze muscles during seizures, minimizing rat discomfort and ensuring immobility during scanning; this also allowed control over breathing rate. Ventilation and blood pressure were monitored closely and if necessary a booster dose (3 mg/kg) of Pancuronium bromide administered. Body core temperature was maintained at 37°C with a heated circulating water pad. The blood pressure, the ventilator and rectal temperature lines were interfaced to a single monitor (Biopak systems, Inc., CA. USA.) and data recorded through out MR scanning.

Rats were placed prone in a stereotaxic holder and a line was placed through the cannula, for convulsant delivery, and extended to a non-MR compatible pump (Cole Pamer 74900 series, Cole-Parmer Instruments, IL. USA) outside the scanner room. This enabled delivery of the drugs while the animal was in the magnet between scans so that slice positioning before and after convulsant could be identical. Each agent, KA, AMPA, ATPA was given to four animals. Ten nanomoles was injected in 5μl saline over five minutes. Four additional animals received normal saline. Convuslant doses were chosen based on a previous study in which rapid seizure initiation had occurred (15). Moreover, each convulsant dose was tested in several animals before the imaging phase of the study was begun, in order to ensure rapid attainment of repetitive stage-4 clinical seizures under direct observation..

To compare the effect of systemic to intra-amygdalar administration, and visualize effect on left and right amygdala without a cannula lesion, four rats received intravenous (*i.v.*) KA, 10–15 mg/kg in a 0.025 mmol/ml solution, administered through a femoral vein line. KA was selected because it is one of the most active Glu-R agonists (16). Two received *i.v.* normal saline.

The experimental protocol required all procedures be terminal and therefore rats were euthanized using 1 ml KCL administered via the arterial lines.

MRI

The MRI experiments were performed on a horizontal bore 7 Tesla scanner operating on a Bruker Avance platform (Bruker Biospin Inc. Bellerica, MA). The rat, with the cannula line attached, was mounted in a 72 mm *i.d.* transmit/receive radio frequency (rf) volume coil for intra-amygdala studies. During intravenous studies, a 25 mm, receive only, surface coil was placed over the head and then mounted on the volume coil which now acted as a transmit coil; the cannula prevented the surface coil use in *i.a.* studies. In order to ensure that the head and neck (region used for ASL) experienced the best magnetic homogeneity, the rat head was positioned in the center of the coil and the performance of the transmit and receive rf coils were optimized.

Three mutually perpendicular scout images were acquired through the brain to localize the cannula site. Subsequently, five 1 mm thick, T_2 weighted axial slices, centered about the cannula, were acquired using a fast spin-echo sequence to delineate anatomical details (Field-of-view [FOV] = 32 mm and matrix size = 256 × 256, in-plane resolution of 125 μm, echo spacing [*TE*] = 10 ms, repetition time [TR] = 2000 ms, echo train length [RARE factor] = 8 and number of averages [NA] = 8, for a total imaging time of approximately 13 minutes; in *i.v.* studies the corresponding amygdela region, to center MR slices, was identified from anatomical literature.

Relative cerebral blood flow was measured using continuous arterial spin labeling (8) in a single 2 mm axial slice containing the amygdala cannula site (Figure 1). A 2 sec. adiabatic labeling pulse (power of 80 mG) was applied at a plane 2 cm caudal (labeling gradient strength = 10 G/cm, label offset ~ 8000 Hz) to the amygdala for spin inversion and thus to label arterial spins. (FOV = 32 mm and matrix size = 64×64, in-plane resolution = 250 μm, TE = 6.8 ms, and TR = 2000 ms, 2 ms delay between labeling pulse and acquisition, total imaging time of approximately 4 min 30 sec). The ASL pulse was followed by a spin-echo imaging sequence. The spin-echo sequence avoided the susceptibility artifacts that may arise from the cannula path in the right side of the brain (Figure 1).

Two baseline ASL image sets were acquired before infusion of drug, and then continuously during and after infusion for an hour. If monitoring of respiration, blood pressure, temperature and blood gases indicated no distress, two more ASL image sets were acquired following

quantitative T_2 and diffusion studies (see below), approximately 100 mins after initial infusion of convulsant or saline. Since T_2 and ADC weighted experiments were not done in *i.v.* studies ASL images were done only for approx. 60 mins. The single coil configuration used in this study allowed only one ASL image to be acquired while preserving temporal resolution under 5 minutes. Therefore, ROIs of ASL images could only be obtained from one slice.

About 60 minutes post infusion, five 1 mm thick, multi echo T_2 weighted (TE=10 ms, number of echos = 16, TR= 3 s, Matrix 128×128, FOV=3.2 cm, experimental time = 16 mins) images from the identical location to morphological images were acquired. DWI were acquired with the diffusion sensitizing gradient applied in one physical (left-right denoted D_x) direction (diffusion gradient duration = 6 ms, 4 b values, 0.7, 379.6, 1379.4, and 3000 mT/m, TE/TR = 32.1/2500 ms, delay between diffusion gradients = 20 ms, matrix 128×128, NA =1, experimental time = 17 mins.); other geometrical parameters were identical to the T_2 images. The T_2 and diffusion weighted images (5 × 1 mm slices) were acquired anterior and posterior to amygdala and hippocampus (beyond either side of the cannula).

The total experimental time for T_2 and DWI was ~33 mins. DWI along one principle axes was acquired to maintain any changes in the acute phase closer to 90 min post infusion. Immediately after the T_2 and DW imaging, another set of ASL images were acquired at about 100 min post infusion.

EEG

We used surface platinum disc (7.2 mm *o.d.*, 4 mm recording diameter, 6 mm high) superficial electrodes applied over each hemisphere with one ground with electro-conductive gel which enabled bipolar recording using AcqKnowledge ™ 3.7 software, (Biopac Systems, Inc, CA. USA.). The electrode assembly did not yield artifact free EEG records while in the scanner. However, in the preliminary tests performed in a separate group of animals before MRI scans were initiated we confirmed that the dosage of convulsant used led to high amplitude epileptiform discharges.

Data Analysis

T_2 and diffusion, and rCBF data were processed and analyzed using software routines written in MATLAB (Mathworks Inc., Natic, MA). T_2 were evaluated by assuming single exponential decay and fitting weighted images into respective relaxation equations. Apparent diffusion coefficients (ADC) maps were calculated fitting the diffusion weighted data to the Stejskal-Tanner equation. The control ASL image (I_C), obtained to compensate for magnetization transfer effects due to interactions with macromolecules in the selected brain slice, and the ASL (I_L) CBF-weighted image were processed to obtain rCBF. We calculated relative blood flow maps corresponding to $([I_C - I_L]/I_C)$ per temporal point. Each rCBF map per 'time point' was then normalized with respect to the average value of the base line (pre-infusion) values. In the relative blood flow images, and for the T_2 and ADC maps, 2.5 mm^2 regions of interest (ROI) were drawn in the left and right basolateral amygdala, hippocampus, basal ganglia, frontal cortex and parietal cortex (Figure 1). The ROI drawn in the right amygdala region in the slice with the cannula was not expected to yield meaningful values. However, this region was used to identify consistently the slices on either side of the cannula, for analysis of T_2 and ADC_x maps,

In order to be able to evaluate drug effects, post-drug administration data were normalized for each animal individually, region by region, to its own baseline (pre-drug) scan. Temporal variation for rCBF, T_2 and ADC were evaluated by averaging data for the left and right hemispheres (2 ROIs) except in amygdala. For a total cortical value, frontal and parietal cortical

values of both hemispheres were also averaged (4 ROIs). Statistical analysis was performed on the average values, using Excel (Microsoft Inc Redmond WA)

Results

Intraamygdalar injection

After infusion of each excitatory amino acid (EAA), CBF increased rapidly throughout the brain (Figure 2A), reaching a peak of 200–300% of baseline levels, with persistent elevation for about 60 minutes (Figure 3). The activation appeared to initiate around 9–14 minutes after infusion of each drug. Summed over all temporal data points, activation was bilateral, and involved neocortical and basal ganglia regions (Figure 2A) as well as hippocampus and amygdala, suggesting secondary generalization of seizure activity (Table 1).

KA produced the highest maximum activation (figures 1 and 3). Left and right hemispheres showed similar activity patterns. The time course for KA activation was more irregular than for other convulsants. Saline showed slightly lower values than unity since there was a decrease in rCBF at some time points. However, the standard deviation for saline remained relatively small, indicating minimal change in rCBF over time.

Average T_2 for cortex (left and right frontal and parietal cortices -4 ROIs) and hippocampus (2-ROIs) for KA were significantly increased (Table 2 and Figure 4a) with respect to saline. AMPA rats had increased cortical but not hippocampal T_2. ATPA rats had no significant T_2 changes. ADC_x cortical and hippocampal KA rat values were significantly reduced (Table 2 and Figure 4b). AMPA and ATPA had no effects compared to saline.

Intravenous injection

In most regions, including thalamic region, rCBF for i.a., varied between 40–75 % above saline baseline (Figure 2B (Table 3). As observed in *i.a.* infusion, activation in *i.v.* infusion was also bilateral. There was no significant difference in overall timing or degree of activation between *i.v.* and *i.a.* KA administration (Table 3).

Physiological monitoring

Over all variation of the blood pressure (BP) for all rats was less than 10% before and after drug infusion (Pre drug = 102.1 ± 6.8 and post drug = 103.6 ± 8.4 mm Hg). Even within a given drug group BP variation over time was less than 10% (data not shown). Body temperature remained relatively constant in all animals (2.5%). Mean blood pH was 7.25 ± 0.27 pre-drug, and 7.37 ± 0.09 for 60–120 minutes post-drug; PO_2 was 143.6 ± 20.6 and 186.3 ± 25.1 and PCO_2 was 31.5 ± 4.5 and 35.1 ± 5.9.

Discussion

Focal amygdalar infusion of glutamatergic agonists lead to rapid and widespread increases in CBF. KA, which activates all GluR, led to greater activation than other agents, and selective GluR5 activation with ATPA a lesser response. The slight variations seen in saline-injected animals may reflect baseline fluctuations of physiological conditions such as BP (17).

Our results are consistent with previous studies of seizures after focal intraamygdalar injections of KA (18) (19). A [(14)C]iodoantipyrine autoradiographic study showed rapid spread of activation from stimulated amygdala to bilateral limbic, cortical, and subcortical structures, with 80–400% CBF increases (20). In the rat maximal electroshock model, peak CBF increases, measured with autoradiographic [C-14] iodoantipyrine, showed a good correlation with circuits underlying variable clinical seizure expression (7). The variability in activation over time for

all animals parallel the widespread, but variable CBF activation seen in patients after ECT as well as animals receiving MES (21).

Anesthesia can affect brain hemodynamics (22). Isoflurane is a vasodilator, and may have affected CBF measurements (23). Two percent isoflurane depressed rat blood pressure, respiration, and heart rates, and increased baseline CBF (17). Isofluorane may have less effect on seizure activity than another alternative, halothane (24). However, both baseline and activated scans were performed under constant anesthesia levels. Isoflurane may have blunted activation, but should not have influenced relative drugs effects or comparison with saline.

Despite a constant infusion rate, variable inter-amygdala diffusion from the cannula tip may have influenced drug effects. However, at any given time point interhemispheric rCBF variation for cortex, hippocampus and thalamus (std. dev. in Table 2) was 25% or less, suggesting relatively uniform drug delivery. Heterogeneity in drug effects might be due to variable excitatory input to inhibitory interneurons. At low doses, ATPA enhances GABAergic transmission in amygdala but causes inhibition at high concentrations (25). It is interesting that ablation of GluR5 receptors reportedly led to higher kainate susceptibility (26). ATPA application to one hippocampus depressed seizure propagation generated in the opposite hippocampus (27).

Other investigators have shown that several convulsants, including KA and pilocarpine, can lead to progressive hippocampal, as well as widespread cortical and subcortical atrophy on MRI (28) (29) (30). Two days after status, increased T_2, and ADC were found in electrically stimulated amygdala, as well as synaptically connected regions such as piriform cortex, midline thalamus, and hippocampus (31). However, increased T_2 relaxation times may not necessarily indicate neuronal injury, and could reflect direct drug toxicity (32) (33).

In pilocarpine-induced status, piriform cortex, amygdala, and retrosplenial (and somatosensory) cortex displayed significant apparent diffusion coefficient (ADC) decreases 12 hours after seizure initiation (34). Reduction in ADC could reflect seizure induced neuronal alterations restricting water motion, akin to ‘swelling’. This might be related to the time when ADC was measured (10) (35). Increased Na^{2+} influx and alteration of membrane homeostasis leading to transient edema during seizures could also decrease ADC (36).

In our study, intraamygdalar injection of GluR agonists evoked bilateral seizure activity and, in the fMRI, increased rCBF. The effect appeared to be greater for KA and AMPA than selective ATPA GluR5 activation. The convulsant doses we used were ‘suprathreshold, having led to to stage four clinical and electrographic seizures in the laboratory. However, we could not record EEG directly, observe seizure activity, or make behavioral observations, in the magnet. Thus, interpretation of our results, particularly the time course and relative intensity of activation produced by each agent, needs to be cautious.

Acknowledgments

The authors wish to thank Dr. Lalith Talagala and Dr. Hyodo Fuminori for the useful discussions and help rendered during the preparation of this manuscript.

References

1. BORTOLOTTO ZA, CLARKE VR, DELANY CM, et al. Kainate receptors are involved in synaptic plasticity. Nature 1999;402:297–301. [PubMed: 10580501]
2. ROGAWSKI MA, KURZMAN PS, YAMAGUCHI SI, LI H. Role of AMPA and GluR5 kainate receptors in the development and expression of amygdala kindling in the mouse. Neuropharmacology 2001;40:28–35. [PubMed: 11077068]

3. HOO K, LEGUTKO B, RIZKALLA G, DEVERILL M, et al. [3H]ATPA: a high affinity ligand for GluR5 kainate receptors. Neuropharmacology 1999;38:1811–1817. [PubMed: 10608276]
4. VIGNES M, CLARKE VR, PARRY MJ, BLEAKMAN D, LODGE D, ORNSTEIN PL, COLLINGRIDGE GL. The GluR5 subtype of kainate receptor regulates excitatory synaptic transmission in areas CA1 and CA3 of the rat hippocampus. Neuropharmacology 1998;37:1269–1277. [PubMed: 9849664]
5. BRAGA MF, ARONIADOU-ANDERJASKA V, LI H. The physiological role of kainate receptors in the amygdala. Mol Neurobiol 2004;30:127–141. [PubMed: 15475623]
6. NOTENBOOM RG, HAMPSON D, JANSEN GH, VAN RIJEN P, VAN VEELEN CW, VAN NIEUWENHUIZEN O, DE GRAAN PN. Up-regulation of hippocampal metabotropic glutamate receptor 5 in temporal lobe epilepsy patients. Brain 2006;129:96–107. [PubMed: 16311265]
7. ANDRE V, HENRY D, NEHLIG A. Dynamic variations of local cerebral blood flow in maximal electroshock seizures in the rat. Epilepsia 2002;43:1120–1128. [PubMed: 12366724]
8. WILLIAMS DS, DETRE JA, LEIGH JS, KORETSKY AP. Magnetic resonance imaging of perfusion using spin inversion of arterial water. Proc Natl Acad Sci USA 1992;89:212–216. [PubMed: 1729691]
9. GROHN O, PITKANEN A. Magnetic resonance imaging in animal models of epilepsy-noninvasive detection of structural alterations. Epilepsia 2007;48 (Suppl 4):3–10. [PubMed: 17767570]
10. ENGELHORN T, WEISE J, HAMMEN T, BLUEMCKE I, HUFNAGEL A, DOERFLER A. Early diffusion-weighted MRI predicts regional neuronal damage in generalized status epilepticus in rats treated with diazepam. Neurosci Lett 2007;417:275–280. [PubMed: 17367928]
11. WIESHMANN UC, SYMMS MR, SHORVON SD. Diffusion changes in status epilepticus. Lancet 1997;350:493–494. [PubMed: 9274593]
12. DIEHL B, NAJM I, RUGGIERI P, et al. Postictal diffusion-weighted imaging for the localization of focal epileptic areas in temporal lobe epilepsy. Epilepsia 2001;42:21–28. [PubMed: 11207781]
13. SZABO K, POEPEL A, POHLMANN-EDEN B, et al. Diffusion-weighted and perfusion MRI demonstrates parenchymal changes in complex partial status epilepticus. Brain 2005;128:1369–1376. [PubMed: 15743871]
14. BAUER G, GOTWALD T, DOBESBERGER J, et al. Transient and permanent magnetic resonance imaging abnormalities after complex partial status epilepticus. Epilepsy Behav 2006;8:666–671. [PubMed: 16503204]
15. STEPPUHN HG, TURSKI L. Modulation of the seizure threshold for excitatory amino acids in mice by antiepileptic drugs and chemoconvulsants. J Pharmacol Exp Ther 1993;265:1063–1070. [PubMed: 8509995]
16. BLEAKMAN D, LODGE D. Neuropharmacology of AMPA and kainate receptors . Neuropharmacology 1998;37:1187–1204. [PubMed: 9849657]
17. SICARD K, SHEN Q, BREVARD ME, SULLIVAN R, FERRIS CF, KING JA, DUONG TQ. Regional cerebral blood flow and BOLD responses in conscious and anesthetized rats under basal and hypercapnic conditions: implications for functional MRI studies. J Cereb Blood Flow Metab 2003;23:472–481. [PubMed: 12679724]
18. BEN-ARI Y, TREMBLAY E, OTTERSEN OP, MELDRUM BS. The role of epileptic activity in hippocampal and “remote” cerebral lesions induced by kainic acid. Brain Res 1980;191:79–97. [PubMed: 7378761]
19. BEN-ARI Y, COSSART R. Kainate, a double agent that generates seizures: two decades of progress. Trends Neurosci 2000;23:580–587. [PubMed: 11074268]
20. CHASSAGNON S, ANDRE V, KONING E, FERRANDON A, NEHLIG A. Optimal window for ictal blood flow mapping. Insight from the study of discrete temporo-limbic seizures in rats. Epilepsy Res 2006;69:100–118. [PubMed: 16503120]
21. BLUMENFELD H, WESTERVELD M, OSTROFF RB, et al. () Selective frontal, parietal, and temporal networks in generalized seizures. Neuroimage 2003;19:1556–1566. [PubMed: 12948711]
22. NAKAO Y, ITOH Y, KUANG TY, COOK M, JEHLE J, SOKOLOFF L. Effects of anesthesia on functional activation of cerebral blood flow and metabolism. Proc Natl Acad Sci U S A 2001;98:7593–7598. [PubMed: 11390971]
23. DUONG TQ. Cerebral blood flow and BOLD fMRI responses to hypoxia in awake and anesthetized rats. Brain Res 2007;1135:186–194. [PubMed: 17198686]

24. MURAO K, SHINGU K, MIYAMOTO E, IKEDA S, NAKAO S, MASUZAWA M, YAMADA M. Anticonvulsant effects of sevoflurane on amygdaloid kindling and bicuculline-induced seizures in cats: comparison with isoflurane and halothane. J Anesth 2002;16:34–43. [PubMed: 14566494]
25. BRAGA MF, ARONIADOU-ANDERJASKA V, XIE J, LI H. Bidirectional modulation of GABA release by presynaptic glutamate receptor 5 kainate receptors in the basolateral amygdala. J Neurosci 2003;23:442–452. [PubMed: 12533604]
26. FISAHN A, CONTRACTOR A, TRAUB RD, BUHL EH, HEINEMANN SF, MCBAIN CJ. Distinct roles for the kainate receptor subunits GluR5 and GluR6 in kainate-induced hippocampal gamma oscillations. J Neurosci 2004;24:9658–9668. [PubMed: 15509753]
27. KHALILOV I, HIRSCH J, COSSART R, BEN-ARI Y. Paradoxical anti-epileptic effects of a GluR5 agonist of kainate receptors. J Neurophysiol 2002;88:523–527. [PubMed: 12091575]
28. WOLF OT, DYAKIN V, PATEL A, VADASZ C, DE LEON MJ, MCEWEN BS, BULLOCH K. Volumetric structural magnetic resonance imaging (MRI) of the rat hippocampus following kainic acid (KA) treatment. Brain Res 2002;934:87–96. [PubMed: 11955471]
29. ROCH C, LEROY C, NEHLIG A, NAMER IJ. Magnetic resonance imaging in the study of the lithium-pilocarpine model of temporal lobe epilepsy in adult rats. Epilepsia 2002;43:325–335. [PubMed: 11952761]
30. NIESSEN HG, ANGENSTEIN F, VIELHABER S, et al. Volumetric magnetic resonance imaging of functionally relevant structural alterations in chronic epilepsy after pilocarpine-induced status epilepticus in rats. Epilepsia 2005;46:1021–1026. [PubMed: 16026554]
31. NAIRISMAGI J, GROHN OH, KETTUNEN MI, NISSINEN J, KAUPPINEN RA, PITKANEN A. Progression of brain damage after status epilepticus and its association with epileptogenesis: a quantitative MRI study in a rat model of temporal lobe epilepsy. Epilepsia 2004;45:1024–1034. [PubMed: 15329065]
32. OSTER J, DOHERTY C, GRANT PE, SIMON M, COLE AJ. Diffusion-weighted imaging abnormalities in the splenium after seizures. Epilepsia 2003;44:852–854. [PubMed: 12790901]
33. DUBE C, YU H, NALCIOGLU O, BARAM TZ. Serial MRI after experimental febrile seizures: altered T2 signal without neuronal death. Ann Neurol 2004;56:709–714. [PubMed: 15389889]
34. WALL CJ, KENDALL E, OBENAUS A. Rapid alterations in diffusion-weighted images with anatomic correlates in a rodent model of status epilepticus. AJNR Am J Neuroradiol 2000;21:1841–1852. [PubMed: 11110536]
35. ENGELHORN T, HUFNAGEL A, WEISE J, BAEHR M, DOERFLER A. Monitoring of acute generalized status epilepticus using multilocal diffusion MR imaging: early prediction of regional neuronal damage. AJNR Am J Neuroradiol 2007;28:321–327. [PubMed: 17297006]
36. WANG Y, MAJORS A, NAJM I, XUE M, COMAIR Y, MODIC NGTC. Postictal alteration of sodium content and apparent diffusion coefficient in epileptic rat brain induced by kainic acid. Epilepsia 1996;37:1000–1006. [PubMed: 8822700]

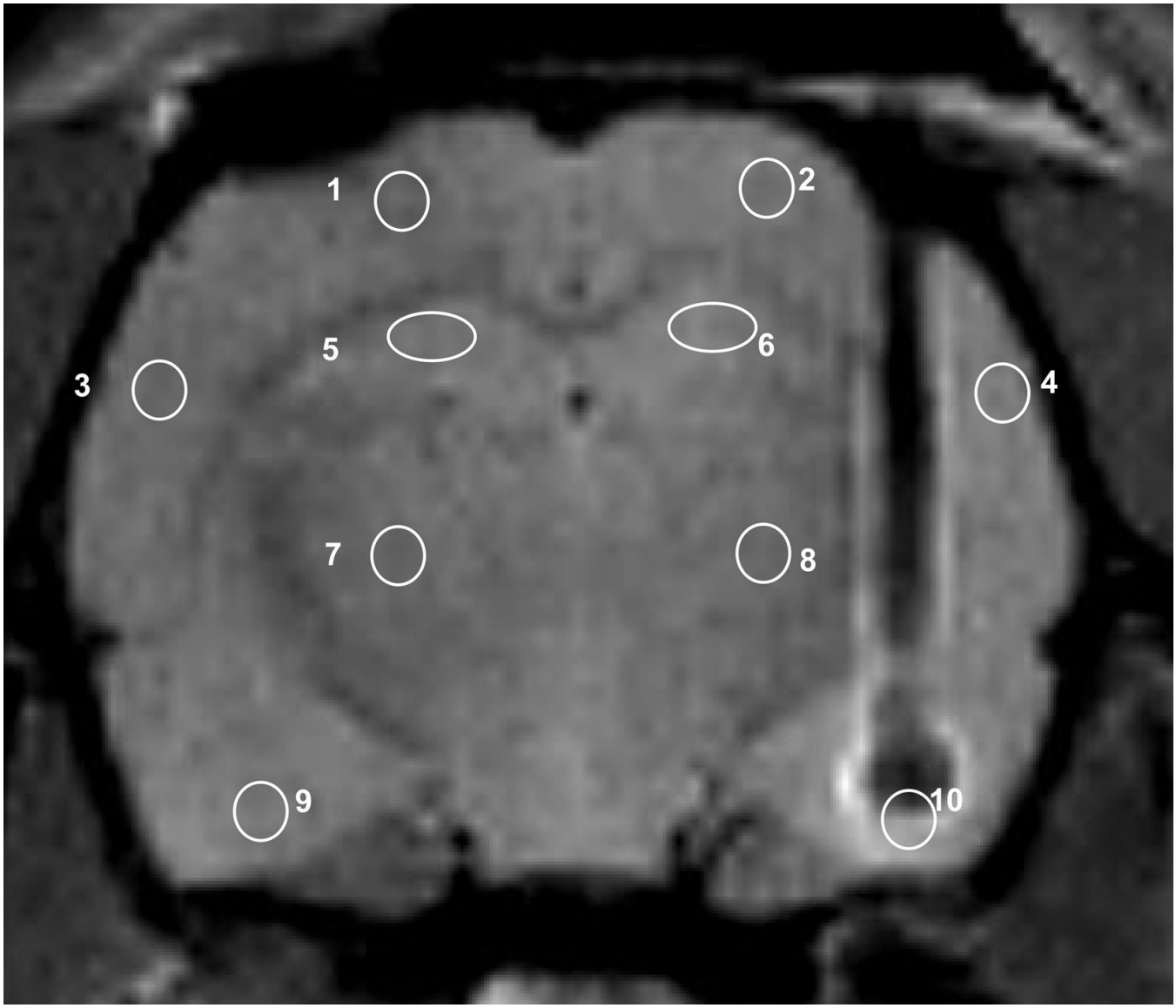

Figure 1.
T_2 weighted axial image of the rat brain showing the intra-amygdalar cannula sites, and the placement of 2.5 mm^2 regions of interest used in data analysis.

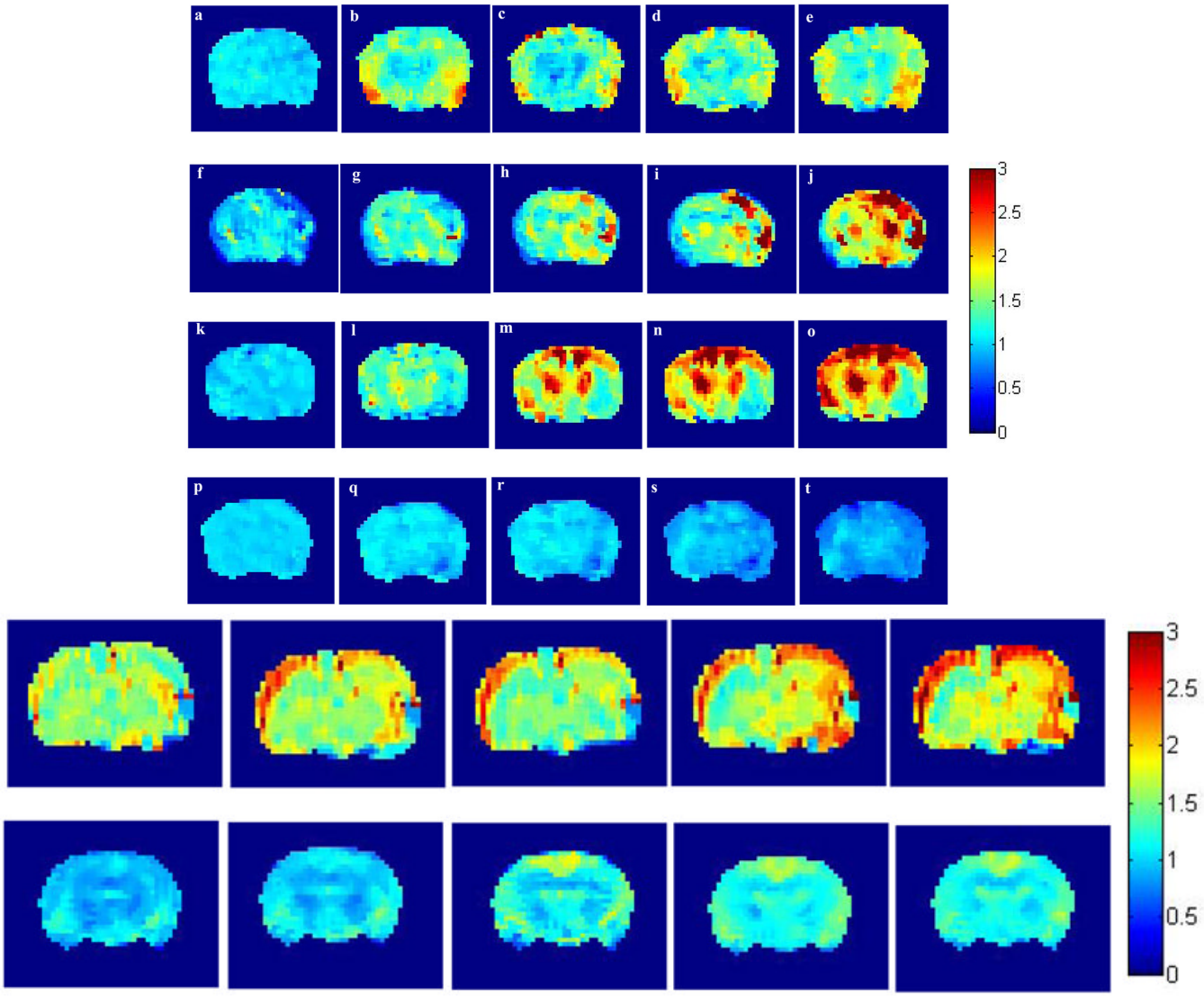

Figure 2.

2A. Effect of intraamygdalar (*i.a.*) infusion of excitatory amino acids and normal saline on cerebral blood flow. Individual animal examples for a–e) ATPA, f–j) AMPA, k-0) KA and p–t) saline acquired at intervals of approx 12–15 mins. The left-hand image in each sequence is the baseline (pre-injection) scan. The color bar shows the range of CBF increases with a maximum of approximately three times baseline.

2B. Effect of intravenous (*i.v.*) infusion of kainic acid and normal saline on cerebral blood flow. Individual animal examples for a–e) KA, f–j) saline acquired at intervals of approx 12–15 mins. The left-hand image in each sequence is the baseline (pre-injection) scan. The color bar shows the range of CBF increases with a maximum of approximately two times baseline.

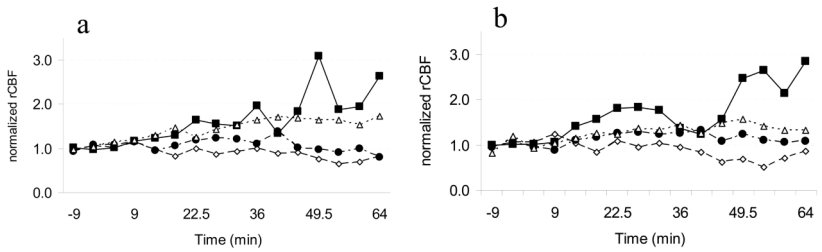

Figure 3.
Temporal variation of rCBF for the three drugs and saline for the a) left and b) right cortical regions. ◇ = Saline, ● = ATPA, Δ = AMPA, ■ = KA.

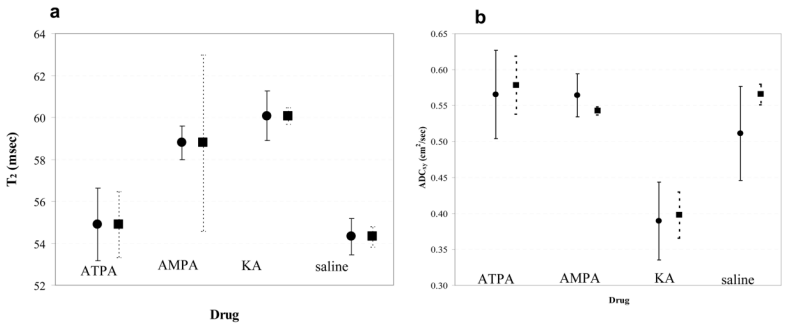

Figure 4.

a) Effect on normalized T_2 values of the ● = cortical area and ■ = hippocampus after approximately 60 minutes after and b) effect on ADC_x values of the, ● = cortical area and ■ = hippocampus approx. 75 mins after intraamygdalar infusion of excitatory amino acids, ATPA, AMPA, KA and normal saline.

Table 1

Mean ± std. dev. % rCBF (normalized to pre-drug) after drug infusion. The rCBF values were averaged over all post-temporal points for a given region (L= Left, R= right)

Drug / **Region**	**Saline**	**KA**	**ATPA**	**AMPA**
L-frontal Cortex	81.1±15.8(112)	194 ± 69.5(338)	104.8±16.2(126)	145.7± 21.6 (172)
R-frontal Cortex	90.6±20.9(129)	192.8± 69.2 (309)	100.7±14.3(132)	107.3 ± 16.9 (132)
L-parietal Cortex	96.4±12.1(119)	150.1± 49.5 (278)	110 ± 16 (149)	152.9 ± 22.1 (182)
R-parietal Cortex	86.5±20.6(118)	160.5± 55.9 (260)	127.3±16.8(151)	150.2 ± 20.9 (181)
L-hippocampus	86.1±14.2(117)	113.7± 26.6 (162)	89.2 ± 8.3 (102)	123.3 ± 18.8 (159)
R-hippocampus	81.2±14.2(107)	147.7 ± 32(189)	102.7± 9.1 (115)	106.5 ± 11.1(123)
L-thalamus	83.3±16.8(108)	127 ± 30 (207)	102.4±15.2(128)	139.4 ± 22.3 (186)
R-thalamus	84.5±12.4(106)	154.6± 42.4 (237)	112.4±10.8(144)	136.7 ± 13.1 (152)
L-amygdala	85.4±14.7(114)	128 ± 21.3 (181)	97.7± 11.4 (117)	134.4± 22.6 (172)

Table 2

T_2 (ms) and ADC (cm^2/sec) along x direction values 60 minutes after convulsant injection. Frontal and parietal cortex, hippocampus, thalamus, left amygdala

Drug	**Saline**		**KA**		**ATPA**		**AMPA**	
T_2/ADC								
ROI	**T_2**	**ADC_x**	**T_2**	**ADC_x**	**T_2**	**ADC_x**	**T_2**	**ADC_x**
Cortex	52.7±1.2	0.51±0.07	56.2±0.8	0.39±0.05	55.05±0.7	0.57±0.06	54.3±1.3	0.57±0.03
Hippocampus	54.3±0.6	0.57±0.01	60.1±0.4	0.4±0.03	54.9±1.6	0.58±0.04	58.8±4.2	0.55±0.1
Thallamus	48.2±0.6	0.58±0.05	50.8±0.4	0.36±0.01	50.9±0.8	0.5±0.05	50.8±2.8	0.5±0.01
Left Amygdala	51.7±4.1	0.60±0.02	56.1±5.1	0.39±0.02	54.7±3.6	0.53±0.07	55.9±4.0	0.57±0.03

Table 3

Mean ± std. dev. normalized rCBF values for *i.a.* and *i.v.* infusion of KA

Drug / **ROI**	**Saline**	**KA i.a**	**KA i.v.**
Cortex	98.68 ± 6.5	174.33 ± 22.44	143.25 ± 9.51
hippocampus	89.9 ± 4.38	130.7 ± 24.04	105.3 ± 5.09
thalamus	86.3 ± 0.57	140.8 ± 19.52	122.4 ± 7.64
Left amygdala	100.3 ± 22.1	128 ± 21.3	124.4 ± 33.9
Right Amygdela	104.4 ± 17.3	-	126.9 ± 34.7